

Spectroscopic Range Points Migration Method for Wide-beam Terahertz Imaging

Takamaru Matsui¹ and Shouhei Kidera^{1,2}

1. Graduate School of Informatics and Engineering, The University of Electro-Communications, Japan

2. Japan Society Science and Technology (JST), PRESTO, Tokyo, Japan.

Abstract—This paper introduces a new spectroscopic imaging method for terahertz (THz) imaging applications. The inherent problem in the conventional THz imaging system is that the azimuth resolution depends on the penetration range due to the lens based dielectric focusing. This problem is efficiently solved by the synthetic aperture (SA) process assuming wider THz beam. Furthermore, the range points migration (RPM) method has a numerous advantages from the usual SA approaches, in terms of accuracy, resolution or computational cost. Moreover, focusing on the feature of RPM, spectroscopic data can be associated to each reflection point. The finite difference time domain (FDTD) based numerical analysis demonstrates that our method accurately reconstructs object boundary with frequency dependent characteristic.

I. INTRODUCTION

There are many promising applications for terahertz (THz) imaging, such as non-destructive testing, or medical imaging applications. General THz imaging systems mostly require dielectric lens to obtain higher azimuth resolution, and then, a possible penetration range with a certain level of azimuth resolution is usually limited. In addition, if the depth of object is unknown, a prior mechanical adjustment of dielectric lens is hardly achieved. For the above problem, the radar approach such as synthetic aperture (SA) process has been considered in many studies [1,2]. However, the SA process requires much expensive computational cost to deal with the full three-dimensional problem, and generates unnecessary responses caused by sidelobe or grating lobe effect. For more efficient radar approach, the range points migration (RPM) method has been developed, in particular for the short range microwave radar [3,4]. The RPM offers a group of scattering center points converted by measured range data, and computationally effective and accurate imaging by suppressing undesirable responses due to the SA process. In addition, the RPM can associate each scattering center to the scattering data, including frequency dependent effect of scattering. Thus, this paper proposes, the RPM based spectroscopic imaging method, where the frequency dependent response are extracted by bandpass filter (BPF) in the pre-processing. The finite difference time domain (FDTD) based numerical simulations demonstrate that the proposed method accurately reconstructs on the target surface at the order of 10 μm , which could not be obtained by the SA imaging process.

II. OBSERVATION MODEL

Figure 1 shows the observation model. It assumes that a homogeneous, low lossy, and non-dispersive media, which

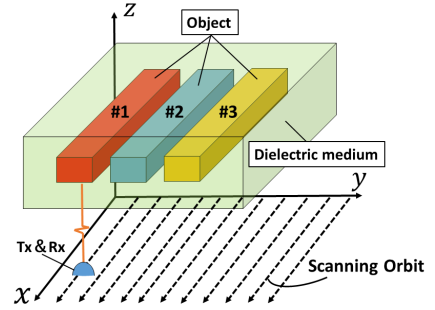


Fig. 1. Observation model.

includes a number of buried objects. A set of transmitter and receiver is scanned, or the array with multiple transmitter and receivers is arranged on the plane. $s(\mathbf{L}, R)$ is defined as an output of an appropriate filter (e.g. matched filter) to a recorded electric field $s(\mathbf{L}, t)$, where $\mathbf{L} = (X, Y, 0)$ denotes the transmitter and receiver location, and $R = ct/2$ is expressed by time t , and c is the speed of light in the air. Range points extracted from the local maxima of $s(\mathbf{L}, R)$ are divided into two groups. One group is defined as $\mathbf{q}_{1,i} = (\mathbf{L}_{1,i}, R_{1,i})$, where each point shows maximum $s(\mathbf{L}, R)$ at R . The remaining range points are categorized into $\mathbf{q}_{2,j} = (\mathbf{L}_{2,j}, R_{2,j})$.

III. SPECTROSCOPIC RPM METHOD

The RPM-based imaging method has been developed to achieve accurate boundary extraction by considering the variance in the scattering center. In the principle of the RPM method, it converts the range point as $\mathbf{q}_{2,i}$, defined as the set of antenna location and measured range, the corresponding scattering center $\hat{\mathbf{p}}(\mathbf{q}_{2,i})$ as:

$$\hat{\mathbf{p}}(\mathbf{q}_{2,i}) = \arg \max_{\mathbf{p}^{\text{int}}(\mathbf{q}_{2,i}, \mathbf{q}_{2,l}, \mathbf{q}_{2,m})} \sum_{j,k} g(\mathbf{q}_{2,i}; \mathbf{q}_{2,j}, \mathbf{q}_{2,k}) \times \exp \left\{ - \frac{\| \mathbf{p}^{\text{int}}(\mathbf{q}_{2,i}; \mathbf{q}_{2,j}, \mathbf{q}_{2,k}) - \mathbf{p}^{\text{int}}(\mathbf{q}_{2,i}; \mathbf{q}_{2,l}, \mathbf{q}_{2,m}) \|^2}{\sigma_r^2} \right\}, \quad (1)$$

where, $\mathbf{p}^{\text{int}}(\mathbf{q}_{2,i}, \mathbf{q}_{2,l}, \mathbf{q}_{2,m})$ is the intersection point among the three orbits of propagation paths, usually determined by the dielectric constant of the background media, and $g(\mathbf{q}_{2,i}; \mathbf{q}_{2,j}, \mathbf{q}_{2,k})$ is weight function considering the sensor separation.

To incorporate the spectroscopic feature into the RPM, the BPF analysis for the reflection data is introduced as follows.

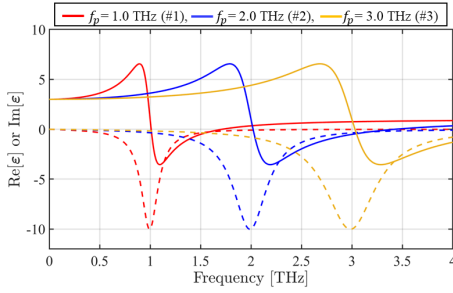


Fig. 2. Lorentz based frequency dependent model of each object. (Solid and broken line denote real and imaginary parts of complex relative permittivity, respectively.)

Here, the BPF with the fixed bandwidth (B), composed of several of different center frequencies f_j , is applied to each received data as $s(\mathbf{L}, t)$. The dominant frequency of reflection as \bar{f} determined for each range point $\mathbf{q}_{2,i}$ as follows:

$$\bar{f}(\mathbf{q}_{2,i}) = \sum_{j=1}^N E_{i,j} f_j / \sum_{j=1}^N E_{i,j}, \quad (2)$$

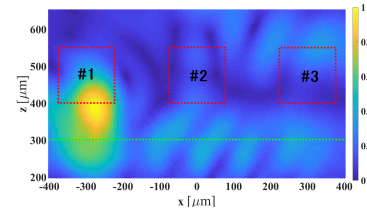
where $E_{i,j}$ denotes of the power density spectrum at f_j after applying BPF to the data of $\mathbf{q}_{2,i}$. Finally, $\bar{f}(\mathbf{q}_{2,i})$ is associated with the scattering center point $\hat{p}(\mathbf{q}_{2,i})$. Note that, this method does not lose the relationship among the antenna location, the range, the dominant frequency and the scattering center, while the SA process lose the above.

IV. NUMERICAL TEST

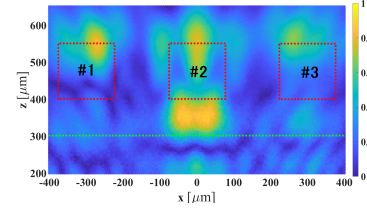
The three-dimensional (3-D) FDTD based numerical example is described as follows. The source current forms a Gaussian-modulated pulse with a center frequency of 2.0 THz and an effective bandwidth of 2.0 THz and is linearly excited along the x -axis. The set of transmitter and receiver is scanned on $z = 0$, where the observation points are equally sampled with 17 points along the x -axis are equally sampled for $-400 \mu\text{m} \leq x, y \leq 400 \mu\text{m}$. The outer dielectric medium is assumed homogeneous and lossy polyethylene terephthalate, with 3.0 relative permittivity and 1.0 S/m conductivity. The buried three objects has a dispersive medium with the Lorentz model [5] as:

$$\varepsilon_r(f) = \varepsilon_\infty + (\varepsilon_s - \varepsilon_\infty) \frac{f_p^2}{f_p^2 + j f \delta_p / \pi - f^2}, \quad (3)$$

where f_p is the resonance frequency, δ_p denotes the damping coefficient, and set as $\varepsilon_s = 3$, $\varepsilon_\infty = 1$, $\delta_p / (2\pi f_p) = 0.1$. Figure 2 shows the frequency dependent model with the different resonance frequency f_p for each object. For the method comparison, Fig. 3 shows the image obtained by the SA process after the BPF with different center frequency is applied. Figure 3 demonstrates that there is frequency dependent responses of SA image, which enables us to spectroscopic imaging. However, it suffers from considerably blurred image due to band limitation of the BPF. On the contrary, Fig. 4 shows the spectroscopic image obtained by the spectroscopic RPM method, namely, the proposed method, and shows that the proposed method associates an accurate boundary point with its spectroscopic quantity. The cumulative probability



(a) BPF from 1.0 to 2.0 THz



(b) BPF from 2.0 to 3.0 THz

Fig. 3. Cross-sectional image obtained by the SA-based method. (Red : Buried object boundary. Blue: Outer medium boundary.)

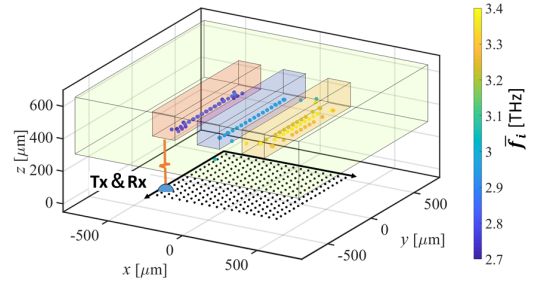


Fig. 4. Spectroscopic image by the RPM method.

of the errors within 0.2λ ($30 \mu\text{m}$) is 96.2% in the proposed method.

V. CONCLUSION

This paper proposed a new spectroscopic imaging method for THz imaging issue, based on the RPM principle. The experimental validation is under our work to demonstrate the effectiveness of our proposed method.

ACKNOWLEDGMENT

This research was supported by JST, PRESTO, Grant Number JPMJPR1771.

REFERENCES

- [1] O'Hara, J. and D. Grischkowsky, "Quasi-optic synthetic phased-array terahertz imaging", *Journal of the Optical Society of America B-Optical Physics*, 2004. 21(6): p. 1178-1191.
- [2] Henry, S.C., et al., "Three-dimensional broadband terahertz synthetic aperture imaging", *Optical Engineering*, 2012. 51(9).
- [3] S. Kidera, et al., "Accurate UWB Radar 3-D Imaging Algorithm for Complex Boundary without Range Points Connections", *IEEE Trans. Geosci. Remote Sens.*, vol. 48, no. 4, pp. 1993-2004, Apr., 2010.
- [4] S. Takahashi and S. Kidera, "Acceleration of Range Points Migration Based Microwave Imaging for Non-destructive Testing", *IEEE Antenna Wireless Propagation Lett.*, vol. 17, no. 4, pp. 702-705, Apr., 2018.
- [5] Z. Li, et al., "Linewidth Extraction From the THz Absorption Spectra Using a Modified Lorentz Model", *Journal of Infrared, Millimeter, and Terahertz Waves*, vol. 34, no. 10, pp 617-626, October 2013.